

# Classical Analysis of Cavity Optomechanics

Eyal Preter, Yan Michalevsky  
Supervised by Eyal Buks

August 27, 2010

## Abstract

We present a classical analysis of a mechanical oscillator subject to the radiation pressure force due to light circulating inside a driven optical cavity. Our analysis is related to the problem of cooling an optomechanical setup to degrees near the ground state of mechanical motion according to quantum theory. Achieving this could provide an insight into quantum phenomena occurring in macro-scale setups. Dynamical backaction based on optical radiation pressure could be employed to reduce thermally excited fluctuations. We review the motion equations system and its steady state solution. We also show numerical simulation results, demonstrating different motion modes of such optomechanical setup.

## 1 Introduction

The possibility to observe quantum mechanical effects in macro-scale systems has fascinated scientists for a long time. But, a significant obstacle on the way is to eliminate the thermal vibrations in the tested setup, which mask or destroy quantum effects. To achieve this, the setup needs to be cooled down to its quantum ground state. For example, the ground state energy of a harmonic oscillator is  $E_0 = \frac{1}{2}\hbar\omega$ . Since it is proportional to the oscillation frequency, we would like, on the one hand, to work with high frequencies to maximize the ground state energy, and on the other hand cool down the setup to make  $E_0$  noticeable on the background of thermal vibrations.

One setup that has been explored for that purpose is an optical cavity with one mirror mounted on a spring (Fig. 1). We study the effects of radiation pressure of photons circulating in the cavity and transferring momentum to the moving mirror. Such research was conducted as early as 1967 by Braginsky and Manukin [1, 2].

In our work we study the effects of the light frequency detuning compared to the cavity resonance frequency. By analytical solution and simulation we show the range of values for which

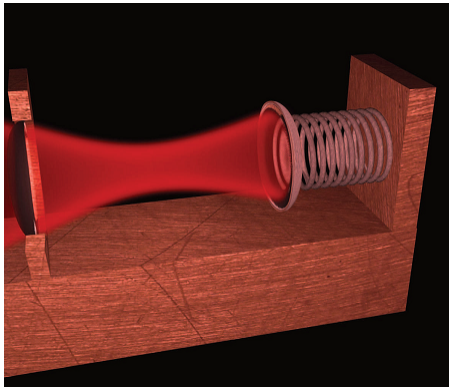


Figure 1: Generic optomechanical system: A Fabry-Perot resonator with one mirror mounted on a spring.

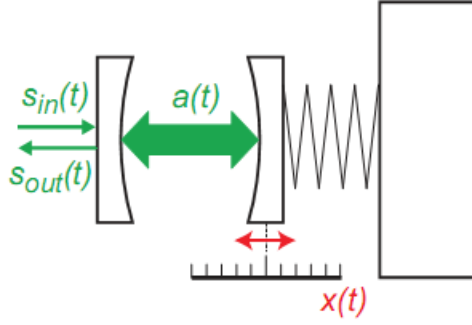


Figure 2: Optomechanical setup - Fabry-Perot resonator with a moving mirror.

self-oscillations of the mirror arise, and the range of detuning values for which the oscillations decay.

## 2 Theoretical Background

### 2.1 Problem Setting

We are dealing with the system depicted in Fig. 2 - a Fabry-Perot resonator with the right mirror mounted on a spring. The field  $s_{in}(t)$ , impinging through the partially transparent left mirror, drives the cavity mode amplitude  $a(t)$ . The right cavity boundary is free to move and its displacement is denoted by  $x(t)$ . We assume that the resonance frequency shift is linearly dependent on the displacement

$$\omega'_c(t) = \omega_c(t) + g_0 x(t)$$

where  $\omega_c$  is the resonance frequency for  $x = 0$  and  $g_0 \equiv \frac{\partial \omega'_c}{\partial x}$ . The resonance frequency of a Fabry-Perot resonator is given by

$$\omega'_c = \frac{\pi c}{L+x} = \frac{\pi c}{L} \cdot \frac{1}{1+\frac{x}{L}} = \frac{\omega_c}{1+\frac{x}{L}}$$

where  $L$  is the distance between the mirrors for  $x = 0$ . For relatively small displacements (compared to  $L$ ) we obtain

$$\omega'_c \cong \omega_c \left(1 - \frac{x}{L}\right)$$

And therefore

$$g_0 = \frac{\partial \omega'_c}{\partial x} = -\frac{\omega_c}{L}$$

#### 2.1.1 Mode Amplitude Response to Moving Cavity Boundary

The equation for cavity mode amplitude is derived from the analysis at Haus[3]. For a monochromatic pump wave  $\bar{s}_{in} e^{-j\omega_1 t}$  we obtain

$$\dot{a}(t) = \left(-i(\omega_c + g_0 x(t)) - \frac{\kappa}{2}\right) a(t) + \sqrt{\eta_c \kappa} \cdot \bar{s}_{in} e^{-j\omega_1 t} \quad (1)$$

$a(t)$  and  $\bar{s}_{in}(t)$  are the amplitudes of the field inside the cavity and the driving field (pump) respectively. They are normalized such that  $|a(t)|^2$  is the intracavity photon number and  $|\bar{s}_{in}(t)|^2$  is the photon flux impinging on the cavity.  $\kappa$  is the energy decay rate, and  $\eta_c$  is the coupling efficiency of the pump [4]. (Note: In quantum analysis of a similar setup  $a(t)$  would be replaced with the annihilation operator  $A$  and  $a^*(t)$  with the creation operator  $A^\dagger$ . Thus,  $|a(t)|^2 = aa^*$  would correspond to the number operator  $N = AA^\dagger$ ).

### 2.1.2 Radiation Pressure Backaction

Now let us examine the effect of radiation pressure on the movable cavity boundary, referred as “backaction”. In case of Fabry-Perot resonator the force acting on the mirror arises from the change of momentum of the reflected photons. The photons have momentum equal to

$$p = \frac{\hbar\omega_1}{c}$$

and therefore

$$\Delta p = 2 \frac{\hbar\omega_1}{c}$$

The force arising from radiation pressure is equal to the change in momentum of a single photons multiplied by the number of photons in the cavity at time  $t$ , times the frequency of collision of each photon with the movable mirror. Since it takes  $\frac{2L}{c}$  for each photon to return to the movable mirror after it was reflected, the collision frequency is given by  $\frac{c}{2L}$ . We obtain

$$\begin{aligned} F_{rp}(t) &= \Delta p \times \text{number of photons} \times \text{collision frequency} \\ &= 2\hbar \frac{\omega_1}{c} |a(t)|^2 \frac{c}{2L} = |a(t)|^2 \frac{\hbar\omega_1}{L} = -\hbar g_0 |a(t)|^2 \end{aligned}$$

The motion equation of the cavity boundary is that of a damped harmonic oscillator

$$\ddot{x}(t) + \Gamma_m \dot{x}(t) + \Omega_m^2 x(t) = \frac{F_{rp}(t)}{m_{eff}} = -\frac{\hbar g_0 |a(t)|^2}{m_{eff}}$$

Transforming to a frame rotating at the laser frequency  $\omega_1$  by substitution of  $\tilde{a}(t) = a(t) e^{-j\omega_1 t}$  in Eq. 1 we get

$$\dot{a}(t) = \left( -i(\omega_c + g_0 x(t)) - \frac{\kappa}{2} \right) a(t) + \sqrt{\eta_c \kappa} \cdot \bar{s}_{in}(t)$$

and we have a coupled system of two differential equations describing the optomechanical behavior of our setup.

## 2.2 Nondimensionalization

The coupled equations describing the optomechanical system are

$$\dot{a}(t) = \left( i(\Delta - g_0 x(t)) - \frac{\kappa}{2} \right) a(t) + \sqrt{\eta_c \kappa} \cdot S_{in}(t) \quad (2)$$

$$\ddot{x}(t) = -\Gamma_m \dot{x}(t) - \Omega_m^2 x(t) - \hbar g_0 \frac{|a(t)|^2}{m_{eff}} \quad (3)$$

where  $\Delta \equiv \omega_1 - \omega_c$  is the frequency detuning.  $\Omega_x$  is the mechanical oscillation resonance frequency,  $\Gamma_x$  is his damping rate and  $m_{eff}$  is his effective mass.

It is convenient to define  $\chi$  and  $\tau$  as dimensionless variables related to  $x$  and  $t$

$$\begin{aligned} \chi &= \mu x \\ \tau &= \Omega_m t \end{aligned}$$

and rewrite equations 2,3 in the dimensionless variables

$$\mu^{-1} \equiv \sqrt{\frac{\hbar \Omega_m}{m_{eff} \Omega_m^2}}$$

$$\begin{aligned}
\tilde{\Delta} &\equiv \frac{\Delta}{\Omega_m}, \quad \tilde{\kappa} \equiv \frac{\kappa}{\Omega_m} \\
\tilde{g}_0 &\equiv \frac{g_0}{\Omega_m}, \quad \tilde{G}_0 \equiv \frac{g_0}{\Omega_m \mu} \\
\tilde{S}_{in} &\equiv \frac{S_{in}}{\sqrt{\Omega_m}}, \quad \tilde{\Gamma}_m \equiv \frac{\Gamma_m}{\Omega_m}
\end{aligned}$$

Using basics differential rules, one finds that  $\frac{d}{dt}\chi = \Omega_m \frac{d}{d\tau}\chi$  and  $\frac{d^2}{dt^2}\chi = \Omega_m^2 \frac{d^2}{d\tau^2}\chi$ . Substitution into Eq. 3 yields

$$\frac{d^2}{d\tau^2}\chi + \tilde{\Gamma}_m \frac{d}{d\tau}\chi + \chi = -\tilde{G}_0 |\tilde{a}(\tau)|^2 \quad (4)$$

where  $\tilde{a}(\tau) \triangleq a\left(\frac{t}{\Omega_m}\right)$ . Now, one can easily do the same for Eq. 2 obtaining

$$\frac{d}{d\tau}\tilde{a} - \left( i\left(\tilde{\Delta} - \tilde{G}_0\chi\right) - \frac{\tilde{\kappa}}{2} \right) \tilde{a} = \sqrt{\eta_c \tilde{\kappa}} \tilde{S}_{in}(\tau) \quad (5)$$

### 2.3 Steady State Solution

For a constant drive amplitude  $\bar{S}_{in}$ , equations 5,4 can be analyzed at first step by finding stable solutions  $\tilde{a}(\tau) = \bar{a}, \chi = \bar{\chi}$  for which all temporal derivatives vanish ( $\frac{d}{d\tau} = 0$ ), requiring simultaneously

$$\bar{a} = \frac{1}{-i\left(\tilde{\Delta} - \tilde{G}_0\bar{\chi}\right) + \frac{\tilde{\kappa}}{2}} \sqrt{\eta_c \tilde{\kappa}} \bar{S}_{in} \quad (6)$$

$$\bar{\chi} = -\tilde{G}_0 |\bar{a}|^2 \quad (7)$$

Using Eq. 6 we find the intracavity photon number

$$|\bar{a}|^2 = \frac{1}{\left(\tilde{\Delta} - \tilde{G}_0\bar{\chi}\right)^2 + 0.25\tilde{\kappa}^2} |\eta_c \tilde{\kappa}| |\bar{S}_{in}|^2 \quad (8)$$

#### 2.3.1 Stability points

Eq. 8 and 7 can be both understood as a function mapping the displacement to an intracavity photon number, as shown in 2.3.1. For any other numerical calculations, the set  $(|\bar{a}|^2, \bar{\chi})$  to be used is the stable solution  $(|\bar{a}|^2, \bar{\chi})$  as given from the first intersection point<sup>1</sup>.

### 2.4 Effective Dumping Coefficient

The dumping induced by dynamical backaction is given by:

$$\tilde{\Gamma}_{eff} \approx \tilde{\Gamma}_m + \frac{1}{2} |\bar{a}|^2 \tilde{G}_0^2 \left( \frac{\tilde{\kappa}}{\left(\tilde{\Delta} + 1\right)^2 + 0.25\tilde{\kappa}^2} - \frac{\tilde{\kappa}}{\left(\tilde{\Delta} - 1\right)^2 + 0.25\tilde{\kappa}^2} \right) \quad (9)$$

Substituting the intracavity photon number with 8 one finds that the effective dumping is related to the frequency detuning  $\tilde{\Delta}$  and to the driving amplitude  $|\tilde{S}_{in}|^2$  is

<sup>1</sup>To find the first real solution of equations 8,7, one needs to find the roots of  $\tilde{G}_0^2 \bar{\chi}^3 - 2\tilde{\Delta} \tilde{G}_0 \bar{\chi}^2 + (\tilde{\Delta}^2 + 0.25\tilde{\kappa}^2) \bar{\chi} + \tilde{G}_0 |\eta_c \tilde{\kappa}| |\bar{S}_{in}|^2 = 0$

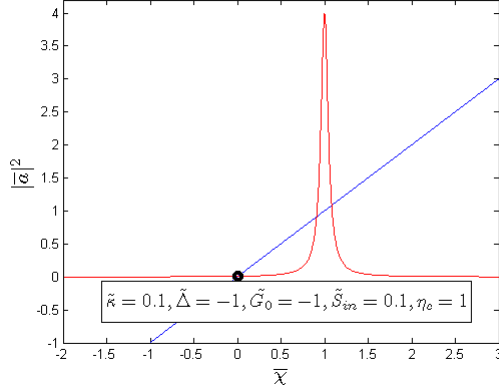


Figure 3: Graphical representation of the coupled equations 7 (blue) and 8 (red). The dotted circle indicates a possible stable solution.

$$\tilde{\Gamma}_{eff} \approx \tilde{\Gamma}_m + \frac{0.5 |\eta_c \tilde{\kappa}| \tilde{G}_0^2}{(\tilde{\Delta} - \tilde{G}_0 \tilde{\chi})^2 + 0.25 \tilde{\kappa}^2} \left( \frac{\tilde{\kappa}}{(\tilde{\Delta} + 1)^2 + 0.25 \tilde{\kappa}^2} - \frac{\tilde{\kappa}}{(\tilde{\Delta} - 1)^2 + 0.25 \tilde{\kappa}^2} \right) |\tilde{S}_{in}|^2 \quad (10)$$

The two areas of interest are where  $\tilde{\Gamma}_{eff}$  is positive and  $\tilde{\Gamma}_{eff}$  is negative.

### 3 Numerical Solution

Different values of  $\tilde{\Gamma}_{eff}$  correspond to different detuning ( $\tilde{\Delta}$ ) and pump amplitude ( $\tilde{S}_{in}$ ) values, and so different points on the graph of  $\tilde{\Gamma}_{eff}$  correspond to different kinds of behavior of the system. To simulate the dynamical behavior of the setup we solved equations 4, 5 numerically for several values of  $\tilde{\Gamma}_{eff}$  (chosen from 4), producing graphs of displacement as a function of time.

Fig. 5, the dotted line shows the steady state displacement as expected for a positive values of effective damping, calculated according to equations 6 and 7. The green crosses show the displacement in the steady state region of the numerical solutions for different values of  $\tilde{\Gamma}_{eff}$ . As expected the numerical solution results are consistent with the analytical solution for steady state. For positive effective damping the oscillations of the mirror decay and the mirror stabilizes in a constant point.

For negative effective damping, the setup goes into self-oscillations stabilizing on a certain amplitude. We can see the amplitude response for negative and positive values of  $\tilde{\Gamma}_{eff}$  in Fig. 6, that demonstrates the amplitude decay and self-oscillations modes.

From 6 we can see that for bigger values of  $\tilde{\Gamma}_{eff}$ , the settling time is shorter. For negative values of  $\tilde{\Gamma}_{eff}$  we can see that where  $|\tilde{\Gamma}_{eff}|$  is bigger, then the self oscillation reach the final amplitude faster. As can be seen in the lower graph in Fig. 4, there are many sets of  $(|\tilde{S}_{in}|^2, \tilde{\Delta})$  with the same value of  $\tilde{\Gamma}_{eff}$ . Every pair differ from the other by the settling time and the final value (or amplitude) of  $\chi$ . Moreover, the temporal reaction of  $|\tilde{a}|^2$  is highly related to  $(|\tilde{S}_{in}|^2, \tilde{\Delta})$ , as illustrated at Fig. 7.

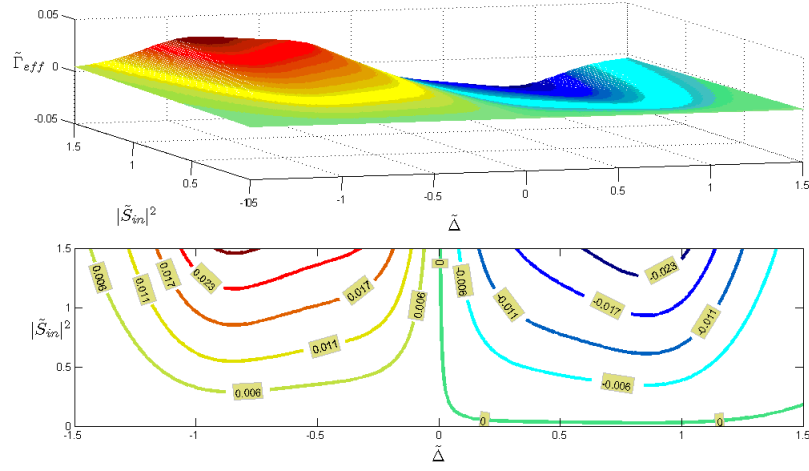


Figure 4: Upper graph:  $\tilde{\Gamma}_{eff}$  as a function of  $\tilde{\Delta}$  and  $|\tilde{S}_{in}|^2$ , according to 10. Lower graph: contours of  $\tilde{\Gamma}_{eff}$ . the right-hand-side of the graph is where  $\tilde{\Gamma}_{eff} < 0$ .

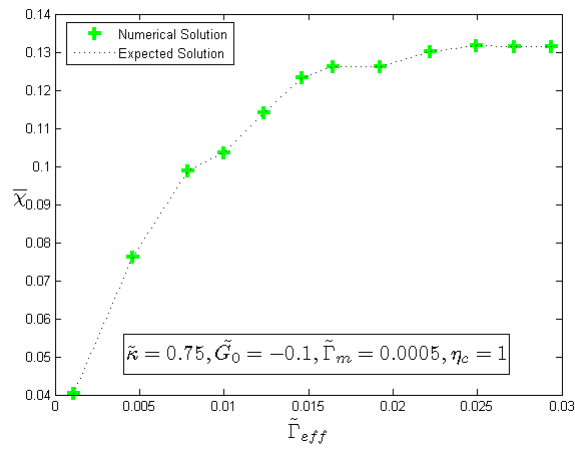


Figure 5: Numerical solution for a positive effective damping.

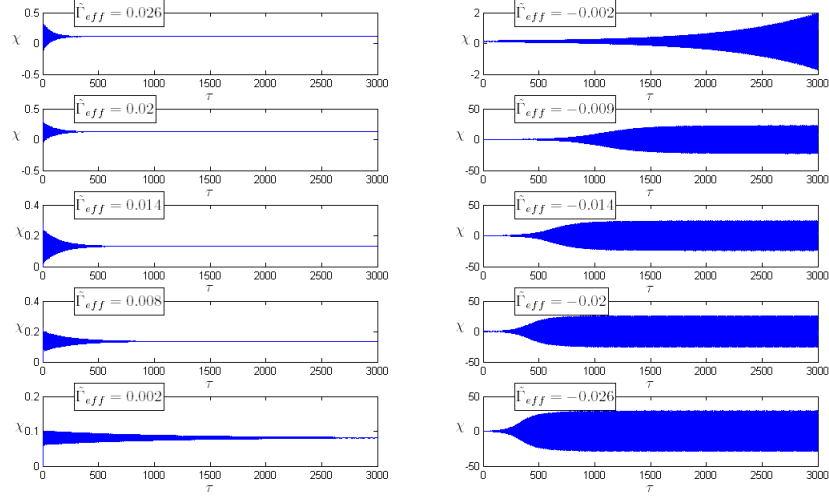


Figure 6: Numerical solution for positive and negative effective damping.

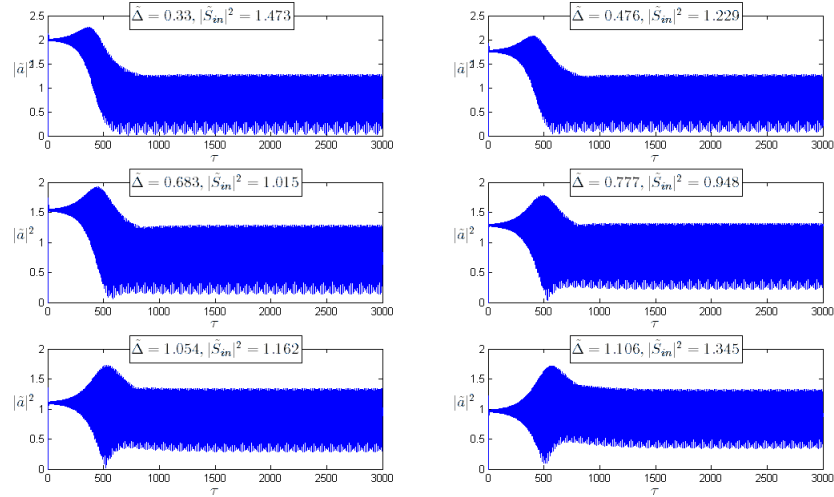


Figure 7:  $|\tilde{a}|^2$  as a function of  $\tau$ , for different values of  $\left(|\tilde{S}_{in}|^2, \tilde{\Delta}\right)$ , at constant  $\tilde{\Gamma}_{eff}$ .  
 $(\tilde{\Gamma}_{eff} = -0.017)$

## References

- [1] VB Braginsky and AB Manukin. Ponderomotive effects of electromagnetic radiation. *Sov. Phys. JETP*, 25:653, 1967.
- [2] VB Braginsky, AB Manukin, and M.Y. Tikhonov. Investigation of dissipative ponderomotive effects of electromagnetic radiation. *Soviet Journal of Experimental and Theoretical Physics*, 31:829, 1970.
- [3] H. Haus. Waves and fields in optoelectronics. *PRENTICE-HALL, INC., ENGLEWOOD CLIFFS, NJ 07632, USA, 1984, 402*, 1984.
- [4] Albert Schliesser and Tobias J. Kippenberg. Cavity optomechanics with whispering-gallery-mode optical micro-resonators. March 2010.